



AMERICAN UNIVERSITY OF BEIRUT

Fuel Cell Hybrid Electric Vehicle Sizing using Ordinal  
Optimization

by

RAFICA KHALED DINNAWI

A thesis

submitted in partial fulfillment of the requirements  
for the degree of Master of Engineering  
to the Department of Electrical & Computer Engineering  
of the Faculty of Engineering & Architecture  
at the American University of Beirut

Beirut, Lebanon

May 2014

AMERICAN UNIVERSITY OF BEIRUT

FUEL CELL HYBRID ELECTRIC VEHICLE SIZING USING  
ORDINAL OPTIMIZATION

by

RAFICA KHALED DINNAWI

Approved by:

\_\_\_\_\_  
[Dr. Sami Karaki, Professor]  
[Electrical and Computer Engineering]

  
Advisor

\_\_\_\_\_  
[Dr. Riad Chedid, Professor]  
[Electrical and Computer Engineering]

  
Committee Member

\_\_\_\_\_  
[Dr. Rabih Jabr, Associate Professor]  
[Electrical and Computer Engineering]

  
Committee Member

Date of thesis defense: May 2, 2014

AMERICAN UNIVERSITY OF BEIRUT

Thesis Form

Student Name: \_\_\_\_\_Dinnawi\_\_\_\_\_Rafica\_\_\_\_\_Khaled\_\_\_\_\_

Master's Thesis       Master's Project       Doctoral Dissertation

I authorize the American University of Beirut to: (a) reproduce hard or electronic copies of my thesis, dissertation, or project; (b) include such copies in the archives and digital repositories of the University; and (c) make freely available such copies to third parties for research or educational purposes.

I authorize the American University of Beirut, **three years after the date of submitting my thesis, dissertation, or project**, to: (a) reproduce hard or electronic copies of it; (b) include such copies in the archives and digital repositories of the University; and (c) make freely available such copies to third parties for research or educational purposes.

---

Signature

Date

## ACKNOWLEDGMENTS

First of all, my sincere appreciation and great gratitude are addressed to my advisor, Prof. Sami Karaki, for his encouragement and assistance in the technical aspects of my graduate study as well as constructive review and comments on my thesis.

I am grateful to my committee members, Prof. Riad Chedid and Prof. Rabih Jabr, for their valuable reviews on my thesis, and encouragement, support, cheerful comments and considerations to me.

Finally, I would like to thank my beloved family, Dad, Mom and my fiancé for their steadfast devotion and love.

# AN ABSTRACT OF THE THESIS

Rafica Khaled Dinnawi

for

Master of Electrical Engineering

Major: Renewable Energy and Power Systems

Title: Fuel Cell Hybrid Electric Vehicle Sizing using Ordinal Optimization

This thesis will develop an optimal design methodology for fuel cell hybrid electric vehicle (FCHEV) based on ordinal optimization (OO) technique and dynamic programming; the optimal design aims to determine the appropriate sizes of the different units – hydrogen tank, fuel cell, and battery – for the purpose of minimizing the investment and operational cost given some specification of the car range, the road type and its gradeability. The dynamic programming simulates the operation of the vehicle for a set of specified sizes on given driving cycles and provides the total vehicle cost per year. The OO method offers an efficient approach for simulation optimization by focusing on ranking and selecting a finite set of good alternatives through two models: the simple model and the accurate model. The OO program sets the sizes of the components to sample the search space using the simple but fast model. In the simple model the operation of components is simplified by taking small samples of the mixed driving cycles with appropriate scaling for the energy utilized. Moreover, the number of discrete states used in the dynamic programming is made relatively low. The OO theory is then applied to determine the numbers of top- $S$  of selected design solutions. The method that is used to determine the best good enough solutions of this selected set  $S$  is the blind pick. Then, the top- $S$  designs are examined using an “accurate model”, which is implemented by taking the whole mixed driving cycles and an increased number of states in dynamic programming. Five different test runs were carried out based on different situations. First, three tests were conducted: one based on gradeability with the variation of the fuel cell and hydrogen costs, another without gradeability, and a third without separate gradeability but with 5% slope on the HWFET driving cycle. Another test run was performed to study the effect of road range. The fifth test run used an OO selection method other than the blind pick. The results presented different optimal sizes in different situations.

# CONTENTS

ACKNOWLEDGMENTS .....	v
ABSTRACT.....	vi
LIST OF ILLUSTRATIONS .....	xii
LIST OF TABLES .....	<b>Error! Bookmark not defined.</b>
NOMENCLATURE .....	<b>Error! Bookmark not defined.</b>
Chapter	
I.INTRODUCTION .....	1
A. Literature Review .....	2
B. Thesis Contribution.....	4
II.SYSTEM COMPONENTS .....	6
A. Vehicle System Model .....	6
1.Modeling of the Vehicle Power Demand.....	7
B. Fuel Cell System Model.....	10
C. Battery Storage.....	13
1.Battery equivalent circuit model .....	15
III.ORDINAL OPTIMIZATION .....	16
A. Ordinal Optimization Procedure .....	19
B. Advantages and Disadvantages of Ordinal Optimization .....	23
2.Advantages.....	23
3.Disadvantages .....	23
C. Discussion of Optimization Methods.....	24
IV. Problem Formulation .....	25
A. Sources of Infeasibility .....	25
B. Relation of Dynamic Programming with Ordinal Optimization.....	26

V. RESULTS .....	29
A. Simulation Data.....	29
B. Test Runs.....	32
1. Test run with variation of Fuel Cell and Hydrogen Costs .....	35
2. Test Run 3.....	39
2. Test Run 4.....	391
2. Test Run 5.....	392
2. Test Run 6.....	393
VI. Conclusion .....	444
References.....	466



## ILLUSTRATIONS

Figure	Page
2.1: System Overview of FCHEV	7
2.2: Vehicle speed and total electric power demand (HWFET) Driving Cycle	9
2.3: Vehicle speed and total electric power demand (UDDS) Driving Cycle with Gradeability	9
2. 4: Fuel cell Block Diagram	10
2.5: Polarization Curve	12
2.6: Fuel Cell Power Current Relation	12
2.7: Fuel Cell Flow Rate Curve	13
2.8: Example of battery charge map for a 40 kW Li-ion battery.	14
2.9: Internal resistanc battery model	15
3.1: Graphical Illustrations of $\Theta$ , G, and S	17
3.2: Five shapes of OPC [16]	18
3.2: Search Space $\Theta$ of N designs to form $\Theta^N$	20
3.3: System Flow Chart	21
3.4: Sample driving cycle	22
3.5: Whole driving cycle	22
5.1: Example of battery charge map for a 40 kW Li-ion battery	31
5.2: Battery charge map scaled curve	31
5.3: Example of instantaneous hydrogen consumption as function of the fuel	32
5.4: Fuel cell scaled per unit flow curve	32

5.5: The UDDS Driving cycle with gradeability at the beginning	35
5.6: Order Performance Curve	43

## TABLES

Table	Page
2.1: Vehicle Data Variables	8
2.2: Fuel cell system parameters	13
3.1: Regressed values of Z1, Z2, Z3, Z4 in Z (k,g) [16]	19
4.1: Samples of Infeasible Results	26
5.1: Base case simulation results	36
5.2 Test run 1 simulation results	37
5.3: Test run 2 simulation results	38
5.4: Comparison table for the best design	38
1.5: Test run 3 simulation results	39
5.6: Comparison table for the best design of test run 3 with the base case	40
5.7: Simulation results for test run 4	41
5.8: Simulation results for test run 5	42
5.9: Comparison table for the best design	42

## NOMENCLATURE

$dt$	Time interval factor between each step i
$J(x)$	Cost function
$I_C$	Investment cost
$G_C$	Glider cost
$O_{Ci}$	Operational cost
$\alpha$	annuity factor
$N$	Number of trips per year=700
$N_1$	Number of trips by UDDS road
$P_{FC}^{max}$	Size for the fuel cell power
$E_{BT}^{max}$	Size for the battery energy
$H_2^{max}$	Size for the hydrogen tank
$P_{Br}$	Brake Power
$P_{FC}$	Fuel Cell Power
$P_D$	Demand Power
$P_{BT}$	Battery Power
$\eta$	Battery efficiency
$E_{CB}$	Energy capacity of the battery
$m_{H2}$	Initial mass of H <sub>2</sub> molecules in the tank
$R_{dFC}$ $R_{uFC}$	Fuel Cell ramp rated limits
$R_{dBT}$ $R_{uBT}$	Battery ramp rated limits
BSS	Battery Storage System
FC	Fuel Cell
SOC	Battery State of charge
$R$	Interest rate=5%
$N$	Depreciation time=15 years

# CHAPTER I

## INTRODUCTION

The fuel cell hybrid electrical vehicle (FCHEV) technologies become a true solution for the traditional vehicles because they use an alternative nontoxic hydrogen fuel. FCHEVs benefit from two sources to supply the power-train demand load: proton exchange membrane fuel cells and batteries or super-capacitors. One issue with these FCHEV is that they consume too much hydrogen. There are many optimization techniques used to achieve the minimum FCHEV cost. The proposed thesis will deal with the ordinal optimization technique to obtain the optimal design of the vehicle. The optimal design aims to determine the good enough sizes of hydrogen tank, fuel cell, and battery for the purpose of minimizing the investment and operational cost. These specific components are examined because their sizing significantly affects vehicle performance, cost and fuel economy.

FCHEVs have been attracting a lot of attention due to the environmental crisis and rapidly rising fossil fuel prices. Fuel cells with proton exchange membranes represent a promising alternative to replace the internal combustion engines used in the transportation sector. In this thesis the influence of fuel cell, battery and hydrogen tank sizing on hydrogen consumption, car mass and economic investment are investigated. These investigations take into account the vehicle drivability requirements on two different types of mixed driving cycles. The ordinal optimization allows a fair comparison, in term of hydrogen consumption for several good sizes on different conditions.

## **A. Literature Review**

Previous studies conducted on FCHEV optimization have mainly focused on limited number of designs. There are a lot of advantages for using FCHEV. One of them is recovering the kinetic energy during regenerative braking [1]. Many optimization techniques exist to achieve the minimum investment and operational cost. An optimized energy management system was developed for FCHVs based on a linear programming technique. This technique led to an efficient power splitting between the energy storage system and fuel cell thus leading to the minimization of hydrogen fuel consumption and operational cost [2]. Linear programming was proposed as a solution for finding the minimum fuel consumption for hybrid propulsion system, and the result may be used to select the component requirements and evaluate control law performance [3].

Other power splitting between the fuel cell (FC) and the battery can be determined by a global optimization algorithm based on optimal control theory [4]. Some papers studied a strategy that quantifies the shifts in the operating point of the FC by using the specific fuel consumption due to load shifting and adapts the conditions for a possible shifting to reduce the total fuel consumption [5].

Ordinal optimization (OO) theory is a method used to efficiently find the good enough solutions with high probability for simulation-based optimization problems [6] & [16]. OO has emerged as an efficient technique for simulation optimization. The OO method has been employed in diverse engineering fields for locating and sizing distributed generation [7].

Some papers studied different topologies types for fuel cell vehicle and hybrid electric vehicle [11]. There are different powertrains topologies for FCHEVs depending on the use and location of the different components of the vehicle. One of the transaction papers provided a detailed comparison for different powertrains topologies. The three topologies are fuel cell-battery, fuel cell-ultracapacitor and fuel cell-battery-ultracapacitor [13]. Argonne National Laboratory researchers worked on plug in hybrid electric vehicles (PHEVs) to reduce the U.S. transportation sector's dependence on petroleum and cut greenhouse gas emissions. They examined two PHEV designs: the power-split configuration and the series configuration [9] & [10].

The components sizing of an FCHEV has been achieved by an optimal power-management strategy, which relies on global optimization algorithm with drive cycle specifications as constraints that limit the fuel cell system and energy storage system (Batteries and super-capacitors) sizes [8]. Different sizes for FC from 35kW as the minimum size to 75kW in steps of 5kW, with 1kW to 8kW in steps of 1 kW for the battery are tested one a specified powertrain topology. Concerning the advantages and weaknesses of a hybridized FCS power source, the sizing procedure for FCHEV has been investigated during the last decade by many researchers [13].

Fuel cell hybrid electrical vehicles can use batteries or ultracapacitor for energy storage. Many papers concentrate their studies on the applications of batteries and ultracapacitors as an energy storage system for different electric vehicles. Such as, charge sustaining and plug-in hybrid-electric vehicles and fuel cell vehicles. This reference proved that fuel cell hybrid vehicles achieved 2-3 times economically higher than that of a gasoline fueled internal combustion vehicle of the same weight and road load [14]. ABVISOR summaries various battery modeling approaches such as lithium

ion (Li-ion), nickel-metal hydride (NiMH), and lead acid. Battery models must be accurate, predict the battery current, voltage and state of charge [15].

The literature review has shown the following gaps. On the level of the optimization technique, previous research disregarded using the ordinal optimization with FCHEVs. Also, as the literature has shown, the use of the OO technique provides a way for the designer to implement a huge number of designs to test their performances and obtain solutions of high quality with much less computational effort than the conventional optimization methods.

## **B. Thesis Contribution**

This thesis will present an ordinal optimization approach for solving the optimal design of FCHEV whereby no previous research has used this technique. While previous studies have focused on either the fuel cell sizes, battery sizes, or both, this study will examine the combination of fuel cell sizes and battery size. In addition, hydrogen tank sizes will be examined because the influence has been disregarded as the literature has shown. The aim is to determine the suitable sizes of the different power units (hydrogen tank, fuel cell, and battery) for the purpose of minimizing the investment and operational cost.

The OO approach consists of three main stages that will enable us to find the best design of FCHEV. During the first stage, a high number of possible alternatives will be uniformly sampled from the large search space. During the second stage, the objective function value and the total cost of FCHEV per year for each of the sampled alternatives will be evaluated using a crude but computationally fast model. The crude model is evaluated in the OO by taking small samples of the mixed driving cycles with



appropriate scaling for the energy utilized to find the top- $S$  solutions with minimum simulation time. The number of the top- $S$  alternatives is determined by the blind pick method. The optimum design is obtained from the combination of the top- $S$  solutions with the good enough solutions “top- $G$ ” as will be discussed in the third chapter on OO. In the field of probabilistic methodologies, a “good enough solution,” means that the solution has a high probability to be a good solution in the top- $S$ . Third, the top- $S$  alternatives from the crude model evaluation are simulated via an accurate model to find the solutions that have a high probability of being in the “good enough” set. OO theory allows computing the size of the selected subset so that it contains one or several designs from among the top good enough samples with a pre-specified alignment probability.

This chapter has examined the available research on fuel cell hybrid vehicles, the FCHEV components, OO and other optimization methods. Research has shown that OO method hasn't been used for applications related to FCHEVs. Thus, this study will use OO to evaluate the performance of huge number of FCHEV designs and find the optimum one in different situations. The next chapter will examine the system components of FCHEV.

## CHAPTER II

### SYSTEM COMPONENTS

This chapter will deal with the system components. The vehicle system model will be discussed with the model of the vehicle power demand, in addition to the fuel cell system model and the battery storage of the vehicle.

#### **A. Vehicle System Model**

This research deals with a hybrid duty vehicle propelled by an AC electric machine. In the base system the hybrid energy source is composed of fuel cell coupled with a lithium ion (Li-ion) battery [9]. Therefore, the system is composed of a fuel cell (FC) as main power source, and the energy storage system (ESS) assists the FC. The system overview of the powertrain architecture corresponds to hybrid architecture as shown in Figure 2.1. The powertrain arrangement integrates a dc/dc converter that is used to couple the FC to the bus, and the ESS is directly connected to the DC bus. A dc/ac inverter is used to power the electric motor. The dc/dc converter and dc/ac inverter are supposed to match the voltages, currents, and power requirement in every time step.

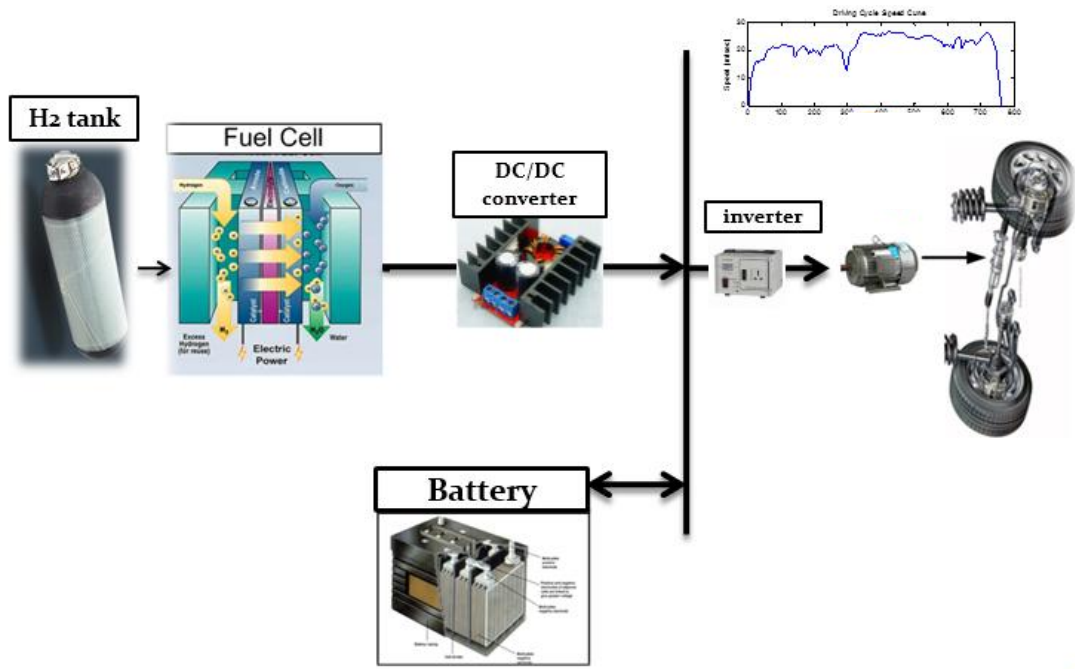


Figure 2. 1: System Overview of FCHEV

### 1. Modeling of the Vehicle Power Demand

The load force of the vehicle consist of aerodynamic drag force  $F_w$  , rolling resistance  $F_r$ , gravitational force  $F_h$  caused by gravity when driving on non-horizontal roads (road slope), and acceleration force  $F_a$ . Hereby, the load power required for vehicle acceleration can be written as follows:

$$P_{load} = \frac{(F_w F_r F_h F_a) V}{\eta_{GB}} \quad (4)$$

Where:

$$F_w = 0.5 \rho A_f C_w V^2 \quad (5)$$

$$F_r = m_v g C_r \cos(\alpha) \quad (6)$$

$$F_h = m_v g \sin(\alpha) \quad (7)$$

$$F_a = m_v a \quad (8)$$

$$V = \omega r \quad (9)$$

The total electric power required from the sources can be expressed as:

$$P_{req} = \frac{P_{load}}{\eta_m \eta_{MI}} \quad (10)$$

The vehicle data variables of the vehicle power demand model are presented in Table 2.1.

Table 2.1: Vehicle Data Variables

Vehicle Data Variables		
$m_v$	Glider mass	915 (kg)
$m_m$	Electric motor mass	90 (kg)
$m_{pe}$	Power Electronics	55 (kg)
$w_p$	Passenger weight	4 × 80(kg)
$g$	Acceleration due to gravity	9.81 (m <sup>2</sup> /s)
$\rho$	Air density	1.21(kg/m <sup>3</sup> )
$A_f$	Frontal Area	2.18 (m <sup>2</sup> )
$C_w$	Aerodynamic Drag coefficient	0.28
$C_r$	Rolling resistance coefficient	0.0075 ( $\Omega$ )
$r_w$	Wheel radius	0.314(m)

In this thesis, the analysis of FCHEV is performed by combining of two standard driving cycles:

- 1) Urban Dynamometer Driving Schedule (UDDS) with and without gradeability
- 2) Highway Federal Emissions Test (HWFET)

These driving cycles are represented by vehicle speeds versus operating time. Figures 2.2 and 2.3 show the vehicle speed and the total electric power demand from sources. The efficiencies for the motor drive line  $\eta_m$  and electric motor and inverter  $\eta_{MI}$  are considered 0.91 and 0.9025 respectively.

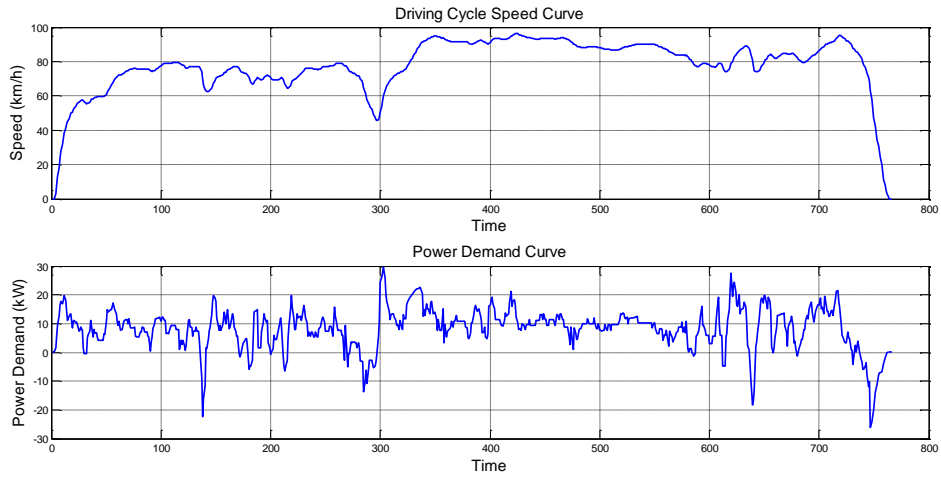


Figure 2.2: Vehicle speed and total electric power demand (HWFET) Driving Cycle

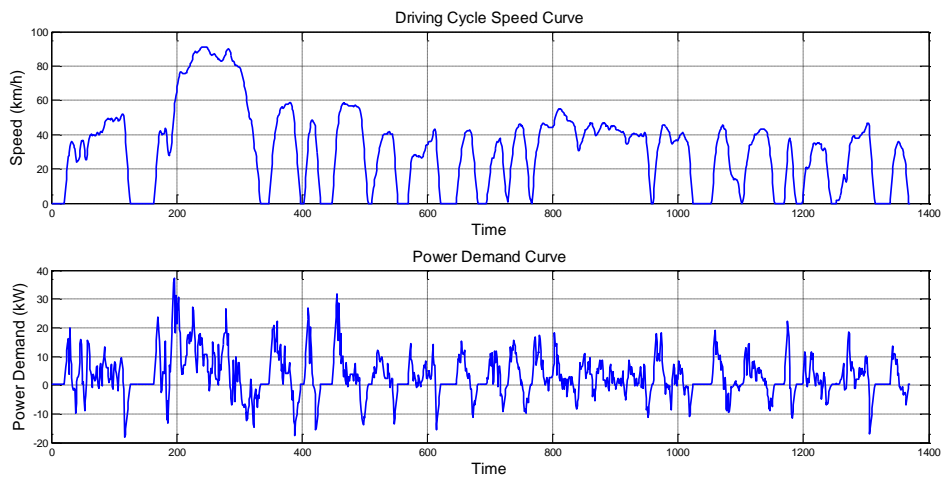


Figure 2.3: Vehicle speed and total electric power demand (UDDS) Driving Cycle with Gradeability

## B. Fuel Cell System Model

Fuel cells are made up of three adjacent segments: anode, electrolyte, and cathode. There are several types of fuel cells, distinguished by the type of the electrolyte material used. For automotive applications, the used type is proton exchange membrane (PEM) fuel cell. PEM is considered for vehicles since it has low temperature operation and faster response (quick start up).

The process begins from the anode side as shown in Figure 2.4. First, hydrogen diffuses from the hydrogen tank connected to the FC (see Figure 2.1) to the anode catalyst and separates into protons and electrons. These protons often react with oxidants causing them to become what are commonly referred to as multi-facilitated proton membranes. The protons are conducted through the membrane to the cathode side, but the electrons are forced to travel in an external circuit (supplying power) because the membrane is electrically insulating. On the cathode catalyst, oxygen molecules react with the electrons (which have traveled through the external circuit) and protons to form water [11].

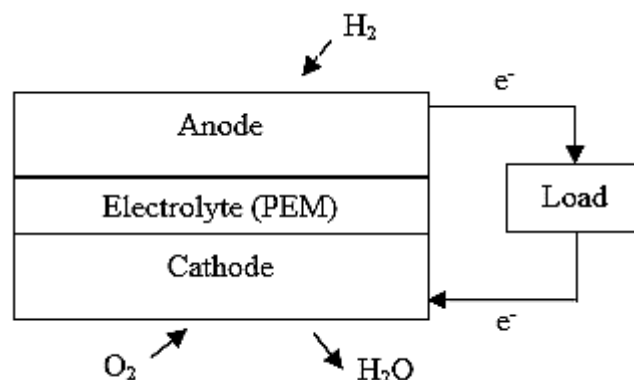


Figure 2. 4 Fuel cell Block Diagram

The fuel cell system is composed of the following: fuel-cell stacks that convert hydrogen and air into electric energy, and a number of auxiliary components. The stack of the fuel cell is composed of cells electrically connected in series under a condition of identical cells. Therefore, the stack voltage  $V_{stack}$  is equal to the number of cells  $N_{cell}$  multiplied by the cell voltage  $V_{cell}$  [11].

$$V_{stack}(i) = N_{cell} \times V_{cell}(i) \quad (1)$$

Under the same condition, the gross stack power is:

$$P_{stack}(i) = V_{stack}(i) \times I \times A_{cell} \quad (2)$$

Where  $I$  is the current density, and  $A_{cell}$  is the cell active area. Table 2.2 summarizes the operating conditions [8]. The fuel cell net power is calculated by subtracting the stack power consumption of the auxiliary components. The auxiliary power has been estimated for the air compressor power consumption (it is the main source of parasitic power).

$$P_{FC}(i) = P_{stack}(i) - P_{aux}(i) \quad (3)$$

In order to calculate the system efficiency suspicious analysis, the rated power is required. Therefore, the overall efficiency of the fuel cells is impacted by the ratio of the parasitic power relative to the stack power output [8] & [12].

The fuel cell hydrogen consumption relation is deduced from the fuel cell power current relation. First, the polarization curve “fuel cell current voltage relation” is plotted. Then, the stack power is calculated in order to plot the fuel cell power current relation which produced from the polarization curve. The amount of hydrogen produced is directly proportional to the fuel cell current. The fuel cell hydrogen consumption relation can be deduced from comparing it with the fuel cell power current relation as shown in Figs 2.6 and 2.7. The characteristic of the fuel cell shows that the maximum

power occurs with the greatest stack current load. For this reason, the fuel cell operates at or below the rated power.

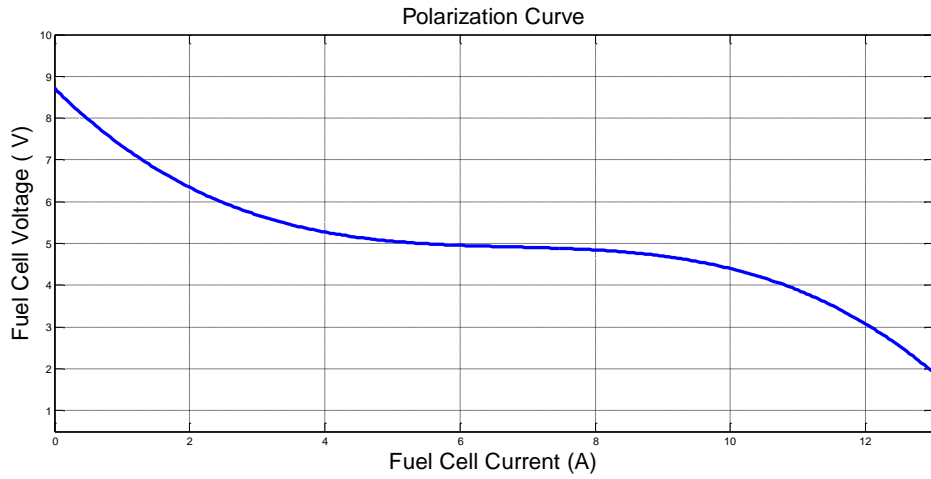


Figure 2.5: Polarization Curve

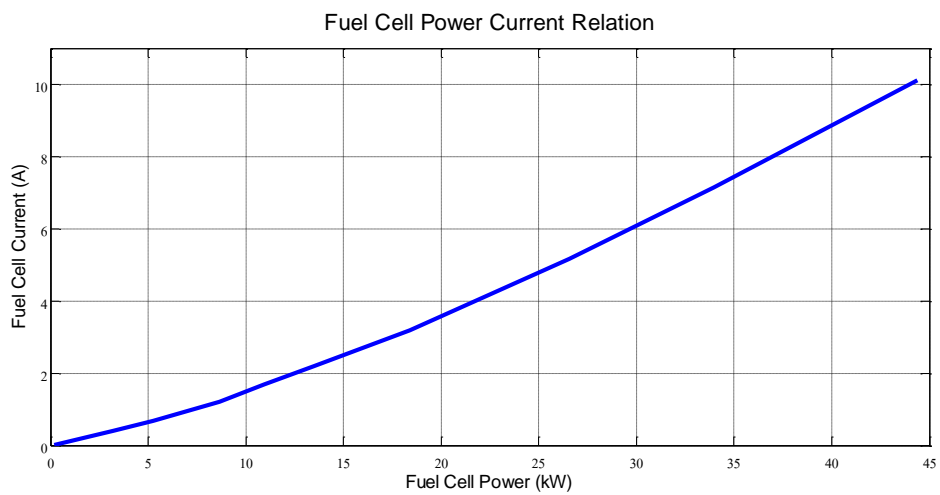


Figure 2.6: Fuel Cell Power Current Relation



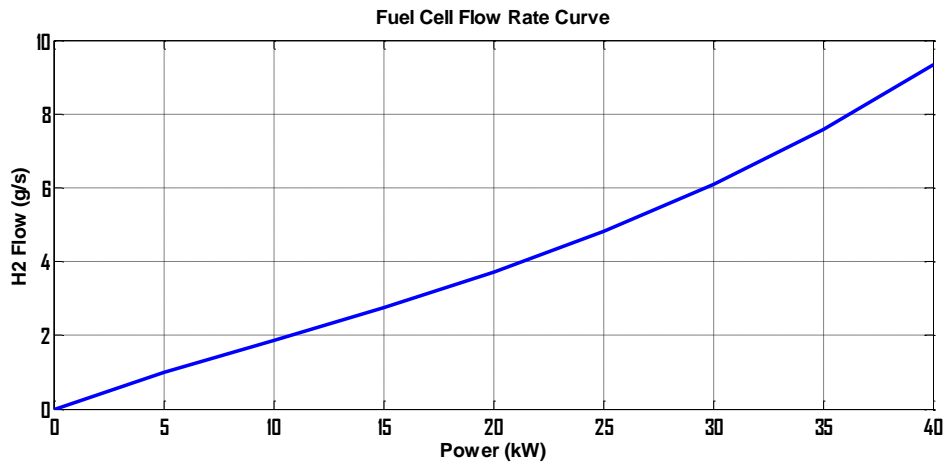


Figure 2.7: Fuel Cell Flow Rate Curve

Table 2.2: Fuel cell system parameters

Cell area	$A_{cell} = 200cm^2$
Maximum current	$1A/cm^2$
Maximum gross power	$544 mW/cm^2$
Maximum net power	$477 mW/cm^2$
Fuel cell system mass	3 kg/kW
Anode pressure	$P_{air} = 1.9 atm$
Cathode pressure	$P_{H_2} = 2 atm$
Stack temperature	$T_{stack} = 80^\circ C$

In the automotive industry applications, a secondary energy storage source is needed to supplement the fuel cell stack such as battery or super-capacitor pack. This is due to the fact that the fuel cell stack is not a stiff power source and, hence, cannot respond to sudden changes in load and system transients. Also, the fuel cell cannot accept the regenerative energy [11]. For this reason, battery storage is used.

### C. Battery Storage

In general, the energy storage system used in FCHEV is either battery or supercapacitor, both of which have significant differences in their electrical characteristics. The lithium-ion batteries are the most established technology in hybrid

vehicle. They are accepted as the optimal choice over nickel-metal-hydrate or lead acid batteries for FCHEVs due to their superior power and energy densities [13]. The focus is on the use of the lithium-ion batteries since it is the future of the FCHEVs [14]. The battery can be charged from the FC or from the network. The battery used in this research is a Li-ion plug in rechargeable battery. It can be fully charged by connecting it to an external electric power source. Therefore, the energy cost (\$/kWh) associated with the battery is calculated by adding investment cost to the cost of electricity purchased from the grid.

The battery charge map may be either measured on a test bench or computed using battery and power converter models. It integrates the power losses induced by the internal resistance [8]. Figure 2.8 represents a 40 kW battery charge map. The model used based on this curve takes into consideration the losses. The battery charge power curve represents a relation between the charge and discharge power of the battery with respect to the internal power of the battery. The following section examines how the battery charge power curve is obtained.

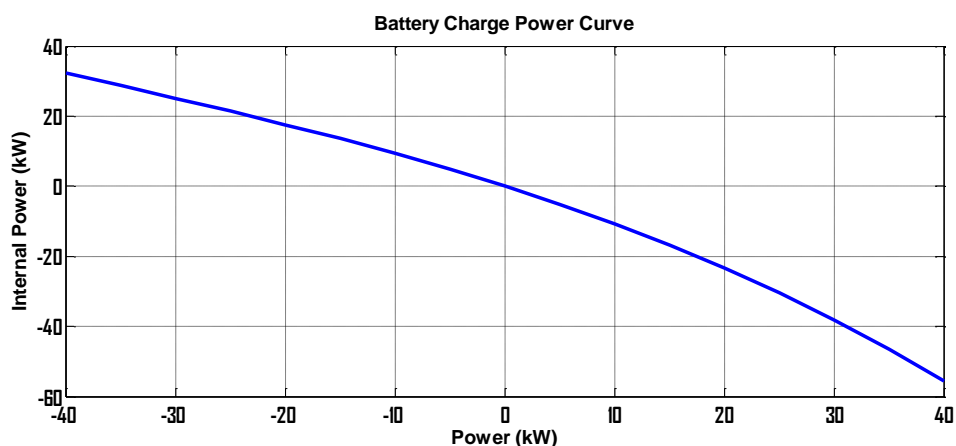


Figure 2.8: Example of battery charge map for a 40 kW Li-ion battery

### 1. Battery equivalent circuit model

The internal resistance model implements an ideal voltage source  $V_{oc}$  to define the battery open-circuit voltage, and a resistance which represents the internal resistance. Both the resistance  $R_o$  and open-circuit voltage  $V_{oc}$  are functions of state of charge (SOC), state of health (SOH) and temperature.  $I_{Batt}$  is the load current with a positive value at discharging and a negative value at charging.  $V_{Batt}$  is the terminal voltage [20]. The curve of the battery charge power can be deduced if the values of the internal resistance in the battery  $R_o$ , current and battery voltage  $V_{Batt}$  are known.

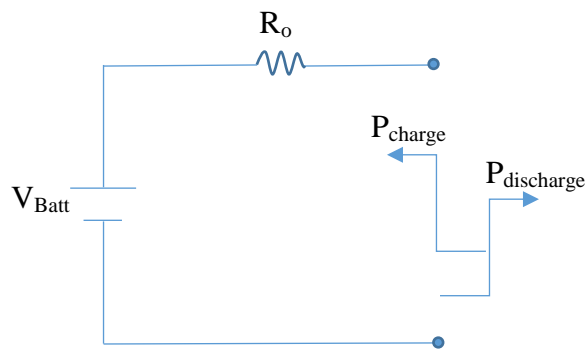


Figure2.9: Internal resistanc battery model

The following chapter briefly discusses the ordinal optimization procedure through FCHEVs, in addition to the advantages and disadvantages for using OO technique.

## CHAPTER III

### ORDINAL OPTIMIZATION

This chapter discusses how ordinal optimization (OO) offers an efficient approach for simulation optimization. OO is based on two tenets stating that the optimization of complex problems can be made much easier:

1. Order comparison: “Order” is much more robust against estimation noise as compared to “value”.
2. Goal softening: For many practical problems, it is enough to settle for a “good enough” solution instead of insisting on getting the “best.”

OO is a technique for finding good enough solutions instead of the best one in a given high alignment probability with less simulation time. Its purpose is not to replace existing techniques for optimization but to complement them.

As an example consider the following minimization problem:

$$\text{Min: } J(x), \text{ where } x \in \Theta$$

$J(x)$  is the objective function which is the cost function in this research;  $x$  is the vector of control variables which represents the different sizes of hydrogen tank, fuel cell, and battery; and  $\Theta$  is the entire set of possible solution space (which is very huge).

A good enough subset  $G(\Theta)$  usually is the top- $g$  designs of  $\Theta$  or of  $N$  which is the subset consisting of the best top  $n\%$  ( $n = 0.1 \sim 5.0$ ) solutions. Since the solution space  $\Theta$  is very huge, a big enough number of samples  $N$ , is used to represent  $\Theta$ . In almost all cases,  $N$  should be equal to 1,000 and more. Therefore,  $g = N * n\%$ . The key point in OO

is to find a Selected Set  $S (\Theta)$  of solutions with an acceptable probability to be a member of the good enough set  $G (\Theta)$  as shown in Figure 3.1. The set of the selected designs in  $N$  is the usually estimated top- $S$  of  $N$ . The method that is used to determine this selected set  $S$ , e.g., it could be blind pick, horse race or other rules using the estimated performance to order the designs (based on a crude model).

For a given alignment probability  $p$  and alignment level  $k$ , the relationship between a selected subset  $S$  and the good enough subset  $G$  should satisfy the following relation:

$$\text{Prob } \{|G \cap S| > k\} \geq p$$

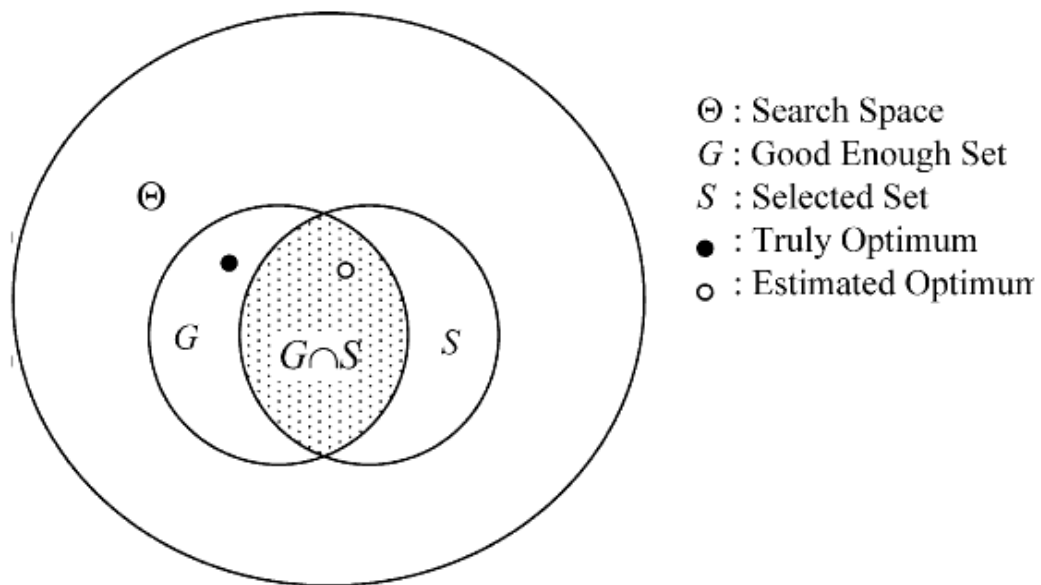


Figure 3.1: Graphical Illustrations of  $\Theta$ ,  $G$ , and  $S$

Another method is used for determining the selected subset size  $S$  by constructing an Ordered Performance Curve (OPC). The OPC is obtained by plotting the values of  $J(x)$  as function of the order of performance, as the best, the second best, and so on. If the optimization is minimizing, then the OPC must be a non-decreasing curve. The five shapes in Figure 3.2 are used to represent five categories of models: 1) Flat: many good schemes, 2) U-shape: many good and bad schemes, 3) Neutral: good and bad schemes

equally distributed, 4) Bell: many intermediate schemes, and 5) steep: many bad schemes. Although obtaining the OPC curve can be complicated, it can be estimated using past experience [16].

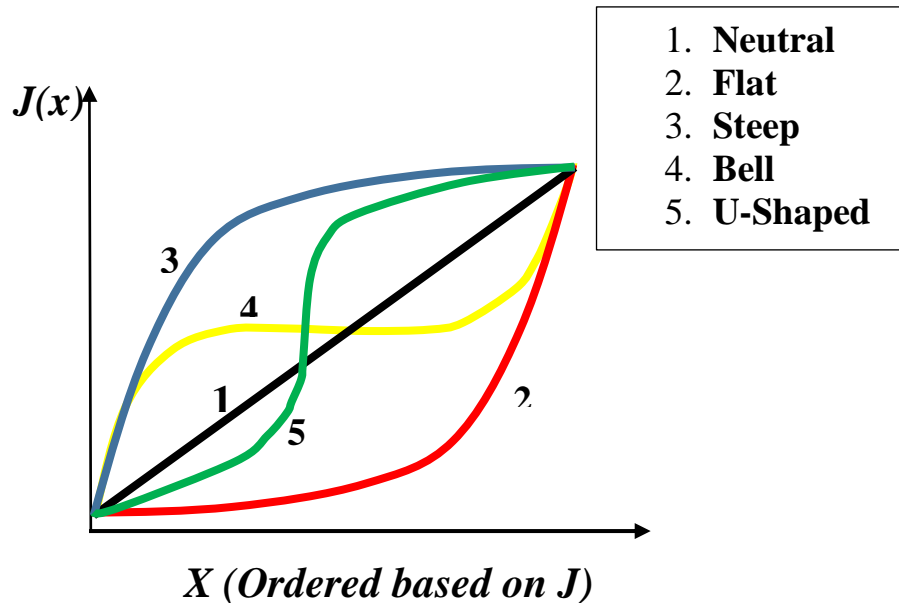


Figure 3.2: five shapes of OPC [16]

After knowing the OPC shape, we can calculate the size  $S$  of the Selected Set  $S(\theta)$  with a given alignment level  $k$ , alignment probability  $p$  and the expected error bound  $W$  using the following equation:

Table 3.1: Regressed values of  $Z_1, Z_2, Z_3, Z_4$  in  $Z(k, g)$  [16]

Noise	$\infty$	$U[-0.5, 0.5]$				
OPC class	B-Pick	Flat	U-shape	Neutral	Bell	Steep
$Z_1$	7.8189	8.1378	8.1200	7.9000	8.1998	7.7998
$Z_2$	0.6877	0.8974	1.0044	1.0144	1.9164	1.5099
$Z_3$	-0.9550	-1.2058	-1.3695	-1.3995	-2.0250	-2.0719
$Z_4$	0.00	6.00	9.00	7.00	10.00	10.00
Noise	$\infty$	$U[-1.0, 1.0]$				
OPC class	B-Pick	Flat	U-shape	Neutral	Bell	Steep
$Z_1$	7.8189	8.4299	7.9399	8.0200	8.5988	7.5966
$Z_2$	0.6877	0.7844	0.8989	0.9554	1.4089	1.9801
$Z_3$	-0.9550	-1.1795	-1.2358	-1.3167	-1.6789	-1.8884
$Z_4$	0.00	2.00	7.00	10.00	9.00	10.00
Noise	$\infty$	$U[-2.5, 2.5]$				
OPC class	B-Pick	Flat	U-shape	Neutral	Bell	Steep
$Z_1$	7.8189	8.5200	8.2232	8.4832	8.8697	8.2995
$Z_2$	0.6877	0.8944	0.9426	1.0207	1.1489	1.3777
$Z_3$	-0.9550	-1.2286	-1.2677	-1.3761	-1.4734	-1.4986
$Z_4$	0.00	5.00	6.00	6.00	7.00	8.00

$$Z(k, g) = e^{Z_1} k^{Z_2} g^{Z_3} + Z_4$$

OO theory ensures that  $S$  contains at least  $k$  good enough designs with a probability level not less than AP ‘alignment probability’.

### A. Ordinal Optimization Procedure

The procedure for the practical application OO to complex optimization problems is summarized as follows:

1. Uniformly sample  $N$  designs from  $\Theta$  to form  $\Theta^N$ . As shown in the following figure.

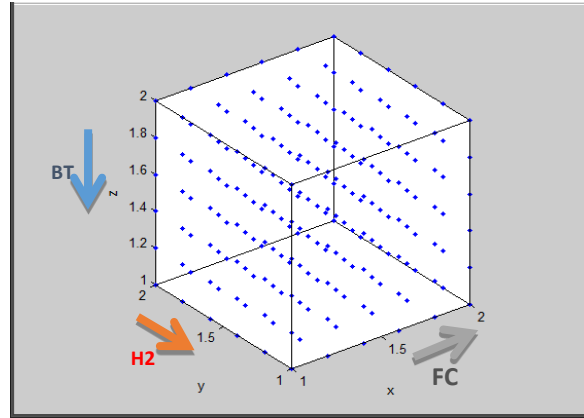


Figure 3.2: Search Space  $\Theta$  of  $N$  designs to form  $\Theta^N$

Step 2: Estimate the performance of the designs in  $\Theta^N$  using a crude model and sort them in ascending order.

Step 3: Plot the Ordered Performance Curve (OPC).

Step 4: Specify the size of the good enough subset,  $g$ , the required alignment level,  $k$ , expected error bound,  $W$ , and alignment probability, AP.

After the results of  $J(x)$  are obtained, the actual good enough alternatives are considered to be the top- $g$  designs in  $\Theta^N$  ( $G=65$ ). Assume  $N=1300$  and the top best is  $n\%$  ( $n = 0.1 \sim 5.0$ ), therefore  $G=N*n\% = 65$ . The alignment probability ( $AP \cong 0.99$ ) that at least one good enough alternative ( $k= 1$ ) is in the selected subset.

Step 5: Use  $Z(k, g) = e^{Z_1 k^{Z_2} g^{Z_3}} + Z_4 = 60$  to determine the size of the selected subset,  $S$ .

Step 6: Select the estimated top- $s$  designs from Step 2 to form the selected subset,  $S$ .

Step 7: OO theory ensures that  $S$  contains at least  $k$  truly good enough designs with a probability level no less than AP.



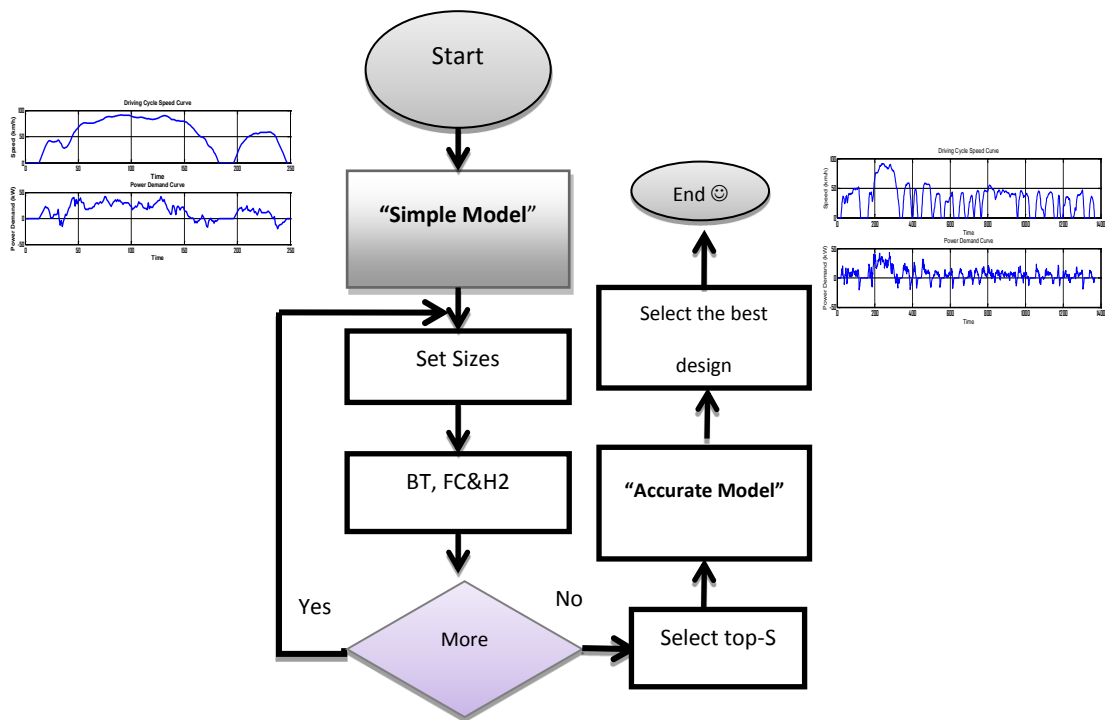


Figure 3.3: System Flow Chart

The figure above represents the scheme flow chart that gives a general idea of the steps followed in this system. The driving cycles in this flow chart shows the difference between the simple model and the accurate one. In the simple model just the part with maximum power demand of the whole driving cycle is chosen.

The crude model is used to estimate the performance of the  $N$  designs. The flow chart in Figure (3.3) demonstrates how the crude, computationally fast, model calculated the cost function of each design in the search space  $\Theta$ . The difference between the crude and the accurate model is the complexity of the car model. But as first approach a bright idea is implemented concerning the driving road cycle. The  $N$  samples is a very huge number, to simulate these samples using the whole driving cycle is very tough and time consuming. Therefore, an energy ratio will be used to get the  $N$  designs simulations on sampled driving cycle with total cost results as if calculated from the whole driving cycle. The total cost for the full road is calculated by dividing the sampled total cost by

the energy ratio. The following two figures represent the sampled and whole driving cycles. From the area under the power demand curve the energy of the sampled and total cycle is calculated. The following equation shows how the energy ratio is calculated.

$$\rho = \frac{E_s}{E_f} \quad C_t = \frac{C_s}{\rho}$$

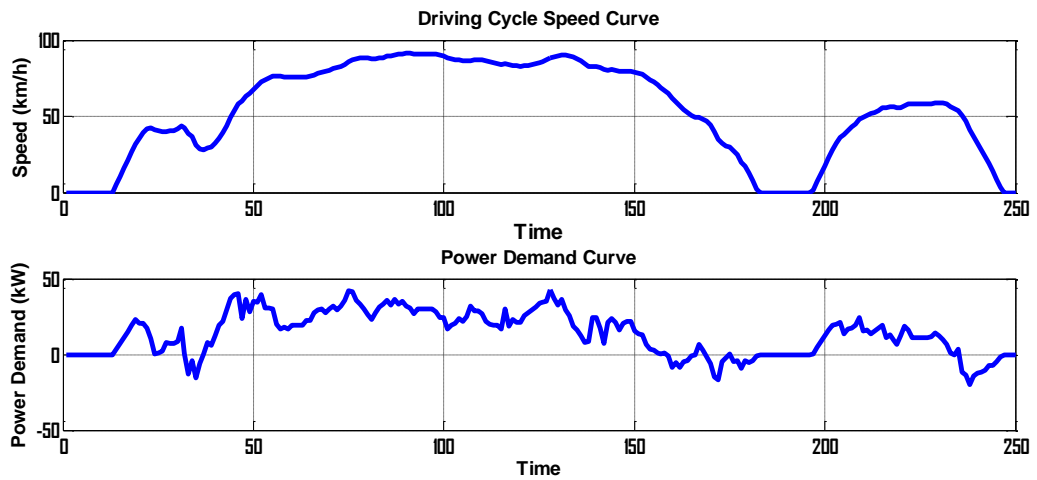


Figure3.4: Sample driving cycle

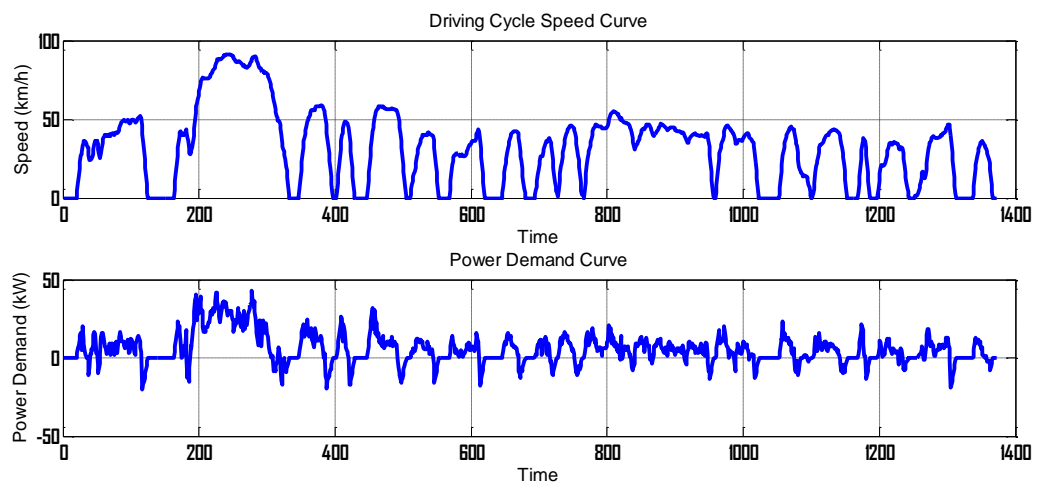


Figure3.5: Whole driving cycle

## **B. Advantages and Disadvantages of Ordinal Optimization**

### **2. Advantages**

The evaluation for the performance of minimum one thousand different designs for FCHEV is time consuming. Optimizing the system performance will mislead a lot of the feasible designs. Ordinal optimization is a technique that tackle this problem in system design by looking at “order” in performances among designs instead of “value” and providing a probability guarantee for a good enough solution instead of the best.

The selection rule, known as the method used to choose the good enough design from the subset designs. There are different selection rules, so the designer can use the one he prefer or use two rules to compare his results and make sure of the accuracy as done in this thesis. Therefore, OO provides this ways to obtain reasonable solutions with less effort.

The influence of bidding strategies can be modeled by simulation, regression, heuristic, game theory and etc... So, one of the most advantages is that ordinal optimization technique can works by any of these models without effecting the performance of the method that allows the crude model to be used in order to quickly determine the good enough bidding strategies [17]. Ordinal optimization can take care of non-linearities and discrete component sizes.

### **3. Disadvantages**

The ordinal optimization is inefficient for system performances of highly peak solutions. OO has limitations as it stands. One key drawback is the fact that the search space  $\Theta$  for many problems can be huge due to combinatorial explosion. Suppose that  $\Theta=10^{10}$  which is small by combinatorial standards. In order to be able to get within the top-1% of  $\Theta$  is still far away from the optimum which can be solved by the hill climbing optimization technique (e.g. non-linear programming).

### **C. Discussion of Optimization Methods**

The hill climbing in traditional optimization techniques can be employed for the systems with the highly peak performances since OO is inefficient for such problems. The OO theory provides a way to obtain solutions of high quality with much less computation effort than the conventional cardinal optimization methods. The OO settles for the “good” solutions with high probability. This deviates from the conventional optimization algorithms, which ask for the best solution for sure. OO is a method for speeding up the process of stochastic optimization problems in different fields.

## CHAPTER IV

### PROBLEM FORMULATION

The problem is formulated as an optimization problem by OO and dynamic programming. The main aim is to find the optimal sizes of the FCHEV components for the purpose of reducing the operational and investment cost. The cost is evaluated for two mixed roads, the Urban Dynamometer Driving Schedule (UDDS) and the Highway Federal Emissions Test (HWFET) driving cycles. The cost ratio of UDDS is taken 0.45 and that of the high way is 0.55.

#### **A. Sources of Infeasibility**

Few results from the crude model solutions fall in infeasibility levels. There are several infeasibility statuses. One of them is due to capacity shortage, when power from the battery and fuel cell is less than the maximum power demand ( $P_{\text{battery}} + P_{\text{fuel cell}} < P_{\text{max demand}}$ ). Other infeasibility level is due to fuel cell level, in this problem the fuel cell is divided into 11 levels in the “simple model”. While in the accurate model the number of levels are 40 levels. If there is a low ramp rate from one of the power sources in the design then this design is infeasible. The sizes of the hydrogen tanks depend on the range of the road which is 240 km. Therefore, every design doesn't match the specified road range it will be considered infeasible.

In order to avoid these infeasibility results from the good enough solutions a penalty factor with large number is added to the objective cost for each infeasible alternative. Optimization problems seek for the lower economic cost. Therefore, after

sorting the results in ascending order, the infeasible solutions will be ignored because they have very high cost due to the applied penalty.

Table 4.1: Samples of Infeasible Results

Hydrogen tank Size (g)	Fuel Cell Size (kW)	Battery Size (kWh)	Cost(\$/yr)	Infeasibility Level
7500	10	3.5	2 334	Low ramp rate
2500	10	1.5	491 040	Capacity shortage
2500	30	3.5	137 633	Design range

### B. Relation of Dynamic Programming with Ordinal Optimization

The cost function  $J(k)$  in \$/year is described as follows:

$$J(k) = \min_k(\alpha I_C(k) + O_C(k)) \quad (1)$$

The investment cost for a given design is determined using the size vectors:

$k = [P_{FC}^{max}, E_{BT}^{max}, H_2^{max}]$ , where the elements are the sizes of the fuel cell, the battery and the hydrogen tank. The optimal design is determined over all the  $k$  designs which has the minimum investment and operation cost. The cost function is used to calculate the total cost of the vehicle per year, so the investment cost is multiplied by the annuity factor  $\alpha$ :

$$\alpha = \frac{r(1+r)^n}{(1+r)^n - 1} \quad (2)$$

The operating cost in \$/trip is calculated by Dynamic Programming for one type of roads and during one trip as described in equation (3).

$$O_{C1}(k) = \sum_{i=1}^T \varphi_{FC}(P_{FC1}(i)) dt + \sum_{i=1}^T \frac{1}{2} \gamma_{BT} \left(1 + \text{sign}(P_{BT1}(i))\right) (P_{BT1}(i)) dt \quad (3)$$

Where

$$\varphi_{FC} = a + bP_{FC} + cP_{FC}^2 \quad (4)$$

Constraints:

$$P_{FC1}(i) + P_{BT1}(i) - P_{Br1}(i) = P_{D1}(i) \quad (5)$$

$$0 \leq P_{FC1}(i) \leq P_{FC}^{max} \quad (6)$$

$$P_{BT}^{min} \leq P_{BT1}(i) \leq P_{BT}^{max} \quad (7)$$

$$R_{dFC}dt \leq P_{FC1}(i) - P_{FC1}(i-1) \leq R_{uFC}dt \quad (8)$$

$$R_{dBT}dt \leq P_{BT1}(i) - P_{BT1}(i-1) \leq R_{uBT}dt \quad (9)$$

$$SOC_{min} \leq SOC_1(i) \leq SOC_{max} \quad (10)$$

$$SOC(i) = SOC_1(i-1) - \varphi_{BT}(P_{BT1}(i)) dt \quad (11)$$

The above equations are used for one type of roads such as the (UDDS) driving cycle as notified by the subscript 1. Similarly, all these equations from (3) to (11) are applied on the (HWFET) driving cycle in order to calculate the total cost per year for the mixed two cycles. The units of  $O_{C1}$  and  $O_{C2}$  are \$/trip1 and \$/trip2 respectively, therefore the total cost per year is:

$$C_{year}(k) = N(0.45 O_{C1}(k) + 0.55 O_{C2}(k)) \quad (12)$$

The above problem is solved using dynamic programming. The power demand forecast curve will be divided into stages. In each stage the fuel cell power level can be in one of several discrete states, which once fixed, for a particular state, allows the battery power to be determined from the power balance constraint (5).

The objective function (3) will be calculated for all the states of stage 1.

Then for each state of subsequent stages the possible transitions from the states of the previous stage are identified, and the minimum cost of reaching each state is built recursively.

When the last stage is reached, the state with minimum cost is recognized, and the preceding states leading to it are identified by a trace-back procedure [19].



## CHAPTER V

### RESULTS

In this chapter two important sections are discussed, which are the simulation data and the test runs section.

#### A. Simulation Data

The ordinal optimization algorithm has been programmed in MATLAB. The objective function that represents the total cost (\$/year) is equal to the investment cost of the components plus the operating cost evaluated using dynamic programming on a \$/year basis as described in equation (1). The car design exercise that we have carried out was done on the glider whose specification were given in Table 2.1. The different sizes that were used in the car design are as follows:

Battery (BT) sizes= [2 4 5 6 7 8 9 10 11 12 13 14 15] (kWh)

Fuel cell (FC) sizes= [5 10 15 20 25 30 35 40 45 50] (kW)

Hydrogen tank (H<sub>2</sub>) sizes= [2 4 5 6 8 10 12 13 14 15] (kg)

The sizes of the hydrogen tanks selected most provide a range of the car which is specified ahead of time. In this design exercise the range specified was 240 km, which has been used in the literature [10]. Other range specifications were also used to study the effect on component sizing. The sizes of the fuel cells and the batteries are chosen according to the peak power demand on the road being considered in the design.

The hydrogen tank cost is between 15 and 18 (\$/kWh), in this research work 17 (\$/kWh) is considered [16]. In order to calculate the hydrogen tank cost in (\$/kWh),

conversion of units is applied from gram to kWh; each one gram is equivalent to 0.016 (kWh). The total battery cost is the price of the unit plus the electricity purchased from the grid. The cost of the battery unit is 400 (\$/kWh) [18]. While the energy battery cost in \$/kWh is 400(\$/kWh). The power battery cost in \$/kW is calculated by dividing the energy battery cost by 11.9(kW/kWh) =33.6 \$/kW. The number 11.9 kW/kWh is deduced from reference [10], in order to convert from kWh to kW and compare the powers between the fuel cell and battery. The cycle efficiency of the battery is around 0.745 calculated at the middle power range and the cost of the electricity from the grid is 0.095 (\$/kWh). Therefore, the cost of electricity purchased from the grid is divided by cycle efficiency then the cost of the electricity used from the battery is 0.1276 (\$/kWh). The fuel cell unit cost is 45 (\$/kW). Moreover, the operational cost is the summation of battery degradation cost plus the hydrogen consumption through the whole year. In this problem the hydrogen cost is considered 0.003 (\$/g). In this problem the number of trips per year is 700 trips based on two trips per day over the length of the year.

The simulation program has two curves the battery charge map which depends on the battery size, and the fuel cell hydrogen consumption curve which depends on the fuel cell size. In OO several sizes are implemented, so a scaled curve is used to get the real curve for every size.

The battery charge map may be either measured on a test bench or computed using battery and power converter models, it integrates the power losses induced by the internal resistance [8]. Figures (5.1) and (5.2) represent the battery charge map for a 40 kW and the battery scaled charged map respectively. The scaled charge map is in per unit of the original curve obtained by dividing each point on the x-axis and y-axis by the maximum power of the battery.

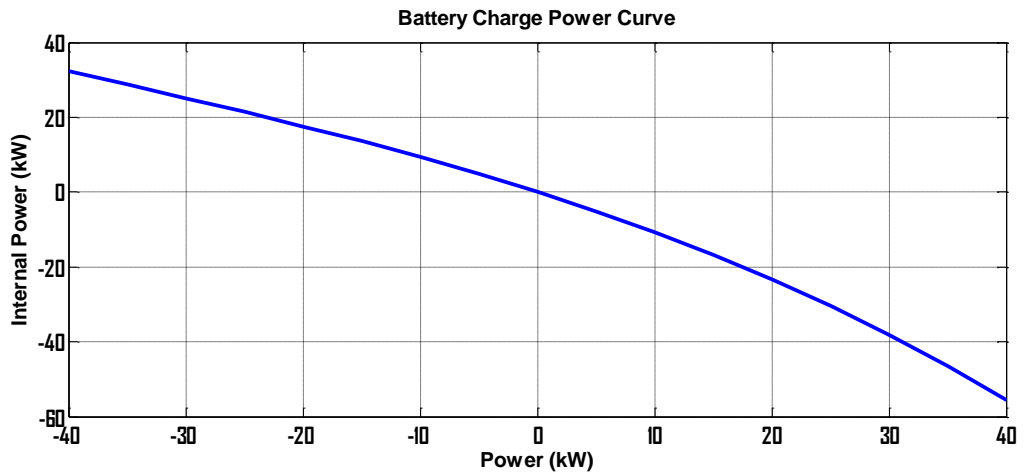


Figure 5.1: Example of battery charge map for a 40 kW Li-ion battery

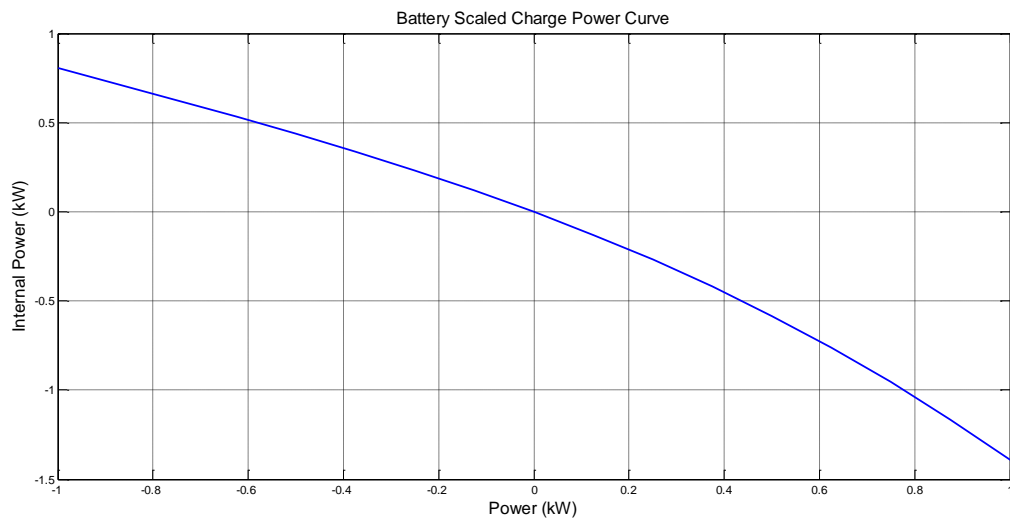


Figure 5.2: Battery charge map scaled curve

The relation between the consumption of hydrogen gram per second and the power of fuel cell in (kW) is shown below in Figure (5.3) for a fuel cell of 40 kW. In OO several sizes of fuel cells are examined, so a scaled curve in per unit for the relation between the consumption of hydrogen gram per second and the power of fuel cell in (kW) is first obtained and used to get the curve for every size, as shown in Figure (5.4).

The fuel cell flow rate curve is converted to a scaled curve by dividing the y-axis and x-axis by the rated fuel cell power. The perunit curve is used to produce the fuel cell flow rate curve for each design by scaling back to the proposed design size.

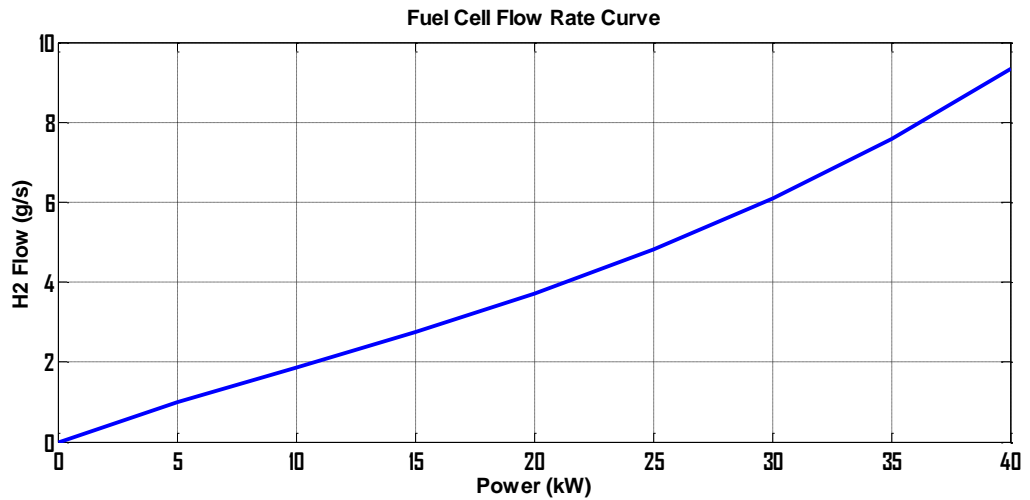


Figure 5.3: Example of instantaneous hydrogen consumption as function of the fuel

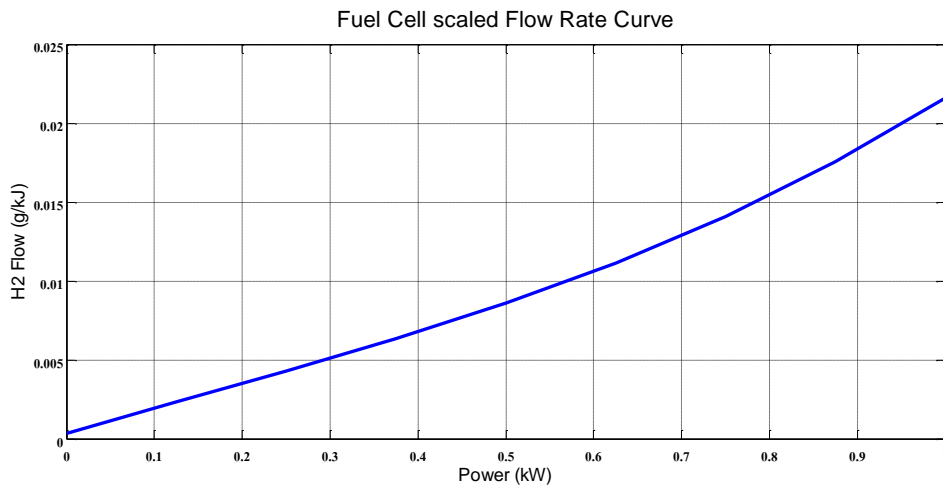


Figure 5.4: Fuel cell scaled per unit flow curve

## B. Test Runs

Seven test runs were carried out based on different situations based on changes in road type, range, gradeability, and OO selection method.

Base Case:

- Gradeability with slope 5% at the beginning of UDDS
- Road range is 240 km
- Fuel cell cost 45 \$/kW
- Hydrogen cost 3 \$/kg
- Selection Method: Blind pick

Test Run 1:

- Gradeability with slope 5% at the beginning of UDDS
- Road range is 240 km
- Fuel cell cost 30 \$/kW
- Hydrogen cost 3 \$/kg
- Selection Method: Blind pick

Test Run 2:

- Gradeability with slope 5% at the beginning of UDDS
- Road range is 240 km
- Fuel cell cost 30 \$/kW
- Hydrogen cost 1.5 \$/kg
- Selection Method: Blind pick

Test Run 3:

- Without-gradeability at the beginning of UDDS
- Road range is 240 km
- Fuel cell cost 45 \$/kW
- Hydrogen cost 3 \$/kg

- Selection Method: Blind pick

Test Run 4:

- Gradeability with slope 5% at the beginning of UDDS
- Road range is 400 km
- Fuel cell cost 45 \$/kW
- Hydrogen cost 3 \$/kg
- Selection Method: Blind pick

Test Run 5:

- Gradeability with slope 5% is added for the full and simple HWFET
- Without-gradeability at the beginning of UDDS
- Road range is 240 km
- Fuel cell cost 45 \$/kW
- Hydrogen cost 3 \$/kg
- Selection Method: Blind pick

Test Run 6:

- Gradeability with slope 5% at the beginning of UDDS
- Road range is 240 km
- Fuel cell cost 45 \$/kW
- Hydrogen cost 3 \$/kg
- Selection Method: Based on Ordered Performance Curve “OPC”

The results presented different optimal sizes in different situations.

### 1. Test run with variation of Fuel Cell and Hydrogen Costs

The number of designs inspected using the simple model is 1300, from which the best 47 were selected according to the blind pick selection method, as discussed in chapter 3. The selected set were examined using the accurate model with gradeability on the UDDS cycle with mixing with the highway driving cycle according to the defined ratios. The gradeability constraint corresponds to the capability of sustaining a constant speed of 110 km/h on a 5% slope. Figure 5.5 shows the UDDS driving cycle speed curve with gradeability in the beginning of the cycle with 110 km/h speed.

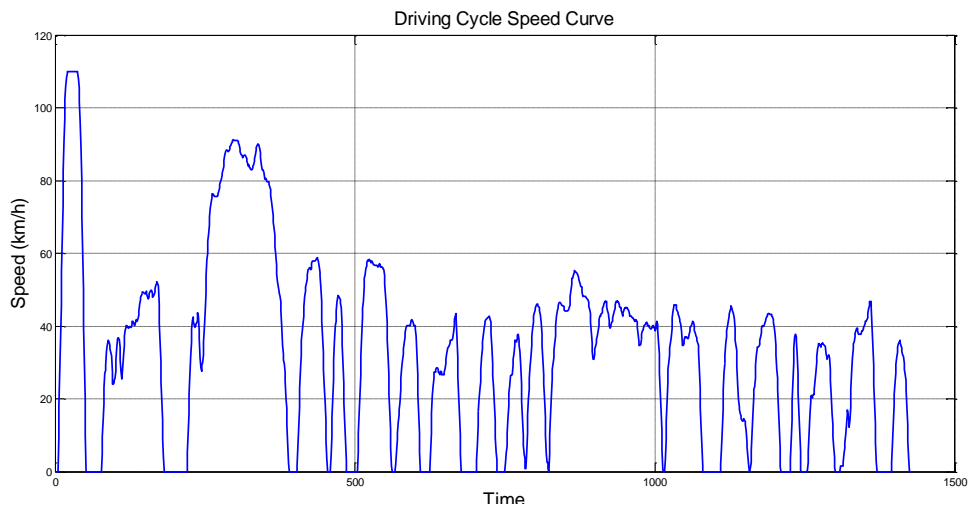


Figure 5.5: The UDDS Driving cycle with gradeability at the beginning

Three test runs, base case, test run 1 and test run 2, are simulated with different hydrogen and fuel cell costs on same mixed driving cycles with gradeability in the beginning of the UDDS cycle and same search space. Base Case takes into consideration the real costs of the fuel cell and hydrogen cost 45\$/kW and 3 \$/kg respectively. In this case the fuel cell cost is larger than the battery cost which is 33.6 \$/kW. As shown from the results of the base case in Table 5.1 the best feasible design

has the sizes of 8000 (g), 45 (kW), 9 (kWh) hydrogen tank size, fuel cell size and battery respectively. In the next two runs the fuel cell cost is reduced to 30 \$/kW which is lower than the battery cost. In Table 5.2 the hydrogen cost is 1.5 \$/kg, while in Table 5.3 it is still 3 \$/kg. This was done in order to study the effect of the hydrogen cost on the design.

Table 5.1: Base case simulation results

Run Number	Hydrogen Tank Size (g)	Fuel cell Size (kW)	Battery Size (kWh)	Investment Cost (\$/yr.)	Operation Cost (\$/yr.)	Total Cost (\$/yr.)	Car Mass (kg)
5	8000	45	9	2429	376	2805	1620
3	8000	30	10	2403	408	2810	1596
6	8000	35	10	2424	396	2820	1606
11	8000	50	9	2451	374	2825	1631
12	8000	40	10	2446	389	2834	1617
18	8000	45	10	2467	383	2850	1628
1	6000	15	11	2324	528	2852	1553
14	8000	25	11	2419	439	2859	1592
16	8000	30	11	2441	418	2859	1603
20	10000	45	9	2481	379	2860	1638
17	10000	30	10	2455	412	2867	1613
21	8000	35	11	2463	405	2867	1614
10	8000	20	11	2398	474	2872	1582
23	10000	35	10	2476	400	2876	1624
30	10000	50	9	2503	377	2880	1649
24	8000	40	11	2484	397	2881	1625
				⋮			
				⋮			
				⋮			
39	8000	5	12	2371	929	3300	1557
29	5000	5	13	2331	978	3310	1538
42	6000	5	13	2357	984	3341	1547
47	4000	5	14	2344	1038	3381	1537

Table 5.1 represents the base case simulation results that are sorted according to the total cost. The first design is considered as the best one with a lower cost than run number 3 and this is expected since the fuel cell size is smaller by 15 kW then it will consume more hydrogen according to the fuel cell power hydrogen consumption curve



in addition to the increase in the battery by 1 kWh. From the top 16 designs the hydrogen tank size vary between 6, 8 and 10 kg. Run numbers 5 and 20 have same power sources sizes but with different hydrogen tank size. The design with the larger tank size leads to an increase in the investment cost while the operation cost remains the same. The last four designs are feasible but with higher operational cost than the first 16 designs.

Table 5.2 Test run 1 simulation results

Run Number	Hydrogen Tank Size (g)	Fuel cell Size (kW)	Battery Size (kWh)	Investment Cost (\$/yr.)	Operation Cost (\$/yr.)	Total Cost (\$/yr.)	Car Mass (kg)
1	8000	45	9	2364	376	2740	1620
4	8000	50	9	2379	374	2753	1631
3	8000	30	10	2359	408	2767	1596
5	8000	35	10	2374	396	2769	1606
6	8000	40	10	2388	389	2777	1617
8	8000	45	10	2403	383	2785	1628
10	10000	45	9	2416	379	2796	1638
19	10000	50	9	2431	377	2808	1649
13	8000	30	11	2398	418	2816	1603
18	8000	35	11	2412	405	2817	1614
12	8000	25	11	2383	439	2823	1592
22	8000	40	11	2427	397	2823	1625
16	10000	30	10	2412	412	2824	1613
21	10000	35	10	2426	400	2826	1624
2	6000	15	11	2302	528	2830	1553
24	8000	45	11	2441	390	2831	1636
			:				
			:				
17	5000	5	12	2286	914	3200	1530
25	6000	5	12	2312	919	3231	1539
27	4000	5	13	2298	973	3271	1529
45	5000	5	13	2324	978	3302	1538

Table 5.3: Test run 2 simulation results

Run Number	Hydrogen Tank Size (g)	Fuel cell Size (kW)	Battery Size (kWh)	Investment Cost (\$/yr.)	Operation Cost (\$/yr.)	Total Cost (\$/yr.)	Car Mass (kg)
1	8000	30	10	2359	252	2611	1596

2	8000	35	10	2374	239	2612	1606
3	8000	40	10	2388	230	2618	1617
4	10000	45	9	2416	219	2635	1638
5	10000	50	9	2431	215	2646	1649
7	8000	30	11	2398	261	2659	1603
9	8000	35	11	2412	246	2659	1614
11	8000	40	11	2427	236	2663	1625
6	8000	25	11	2383	282	2665	1592
10	10000	30	10	2412	255	2667	1613
12	10000	35	10	2426	242	2668	1624
14	10000	40	10	2440	232	2673	1635
16	10000	45	10	2455	225	2679	1646
8	8000	20	11	2369	316	2685	1582
17	10000	50	10	2469	220	2689	1657
20	12000	50	9	2483	217	2700	1667
				:			
				:			
22	6000	10	12	2326	548	2874	1550
37	5000	10	13	2339	579	2918	1549
27	4000	5	12	2260	828	3087	1521
38	5000	5	12	2286	833	3118	1530

The hydrogen tank used are in the ranges of 8 kg and 10 kg and sometimes reaches 12 kg as shown from the top 16 results of Table 5.3. On the other hand, hydrogen tank sizes used with the designs of Table 5.2 vary between 8 kg and 6 kg. This difference is due to the effect of the hydrogen cost.

Table 5.4 summaries the first designs of the base case, test run 1 and test run 2 by showing the difference between the annual costs and power sources sizes.

Table 5.4: Comparison table for the best design

	<b>Hydrogen Tank Size (g)</b>	<b>Fuel cell Size (kW)</b>	<b>Battery Size (kWh)</b>	<b>Investment Cost (\$/yr.)</b>	<b>Operation Cost (\$/yr.)</b>	<b>Total Cost (\$/yr.)</b>	<b>Car Mass (kg)</b>
a	8000	45	9	2429	376	2805	1620
b	8000	45	9	2364	376	2740	1620
c	8000	30	10	2359	252	2611	1596

- a) Base Case
- b) Test Run 1
- c) Test Run 2

The difference between the base case and test run 1 is the fuel cell cost, to study the effect of the battery costs if it is lower than the fuel cell cost. The unit sizes remain the same in the two cases; therefore, the investment cost decreases since the fuel cell unit cost decreases as shown from the comparison of the Tables 5.4. Test run 2 considers the hydrogen cost 1.5 \$/kg; therefore, the fuel cell decreases to 30 kW and the car cost and mass decreases as a compared to the base case and test run 1.

## 2. Test run 3

This test run is done to compare the performance and the power sources sizes of the vehicle if it is driven on a road without gradeability. The table below shows the results of mixed roads without gradeability under same condition of the base case with the difference of gradeability. As recognized from the results that unit sizes dropped down. The maximum fuel cell size from the top 16 designs shown below is 10 kW and with respect to the battery is 4 kWh. Therefore, the car cost depends on its application. A design with the sizes of 5000 g, 10 kW and 4 kWh hydrogen tank, fuel cell and battery can be perfect for city car where no need for gradeability.

Table 2.5: Test run 3 simulation results

Run Number	Hydrogen Tank Size (g)	Fuel cell Size (kW)	Battery Size (kWh)	Investment Cost (\$/yr.)	Operation Cost (\$/yr.)	Total Cost (\$/yr.)	Car Mass (kg)
3	5000	10	4	2007	306	2314	1478
5	6000	10	4	2033	308	2341	1487
12	8000	35	2	2117	251	2368	1544
19	8000	40	2	2139	254	2392	1555
9	8000	10	4	2086	310	2396	1505
14	8000	15	4	2107	292	2399	1516
22	8000	20	4	2129	280	2409	1527
8	6000	10	5	2072	341	2413	1495

23	8000	45	2	2160	257	2418	1566
25	10000	35	2	2169	253	2422	1562
24	8000	25	4	2151	274	2425	1538
29	8000	50	2	2182	262	2443	1577
33	8000	30	4	2172	272	2444	1549
36	10000	40	2	2191	256	2446	1573
16	10000	10	4	2138	313	2451	1523
28	10000	15	4	2160	294	2454	1534
				:			
				:			
				:			
41	4000	5	9	2152	589	2740	1498
1	4000	5	5	2399	391	2389	1466
2	5000	5	5	2457	393	2417	1475
4	6000	5	5	2518	395	2445	1484

Table 5.6: Comparison table for the best design of test run 3 with the base case

	<b>Hydrogen Tank Size (g)</b>	<b>Fuel cell Size (kW)</b>	<b>Battery Size (kWh)</b>	<b>Investment Cost (\$/yr.)</b>	<b>Operation Cost (\$/yr.)</b>	<b>Total Cost (\$/yr.)</b>	<b>Car Mass (kg)</b>
a	8000	45	9	2429	376	2805	1620
b	5000	10	4	2007	306	2314	1478

a) Base Case  
b) Test run 3

The above table shows that without gradeability the total cost and the vehicle mass drop by 17.5% and 9% respectively. As shown the fuel cell size decreases from 45 kW to 10 kW, battery drops to 4 kWh and the hydrogen tank becomes 5 kg. The reason of this change is that with gradeability the maximum load demand for the mixed roads is 128.31 kW while without gradeability it is 37.3 kW.

### 3. Test run 4

Different road ranges should be taken into consideration in order to study the effect of the hydrogen tank size used in the vehicle. The base case is based on road range of

240 km. As deduced from the shown table that the hydrogen tank sizes increase from 6 kg to 10 kg as compared to the base case. If a comparison is done between the road ranges of 400 km and 240 km, a conclusion can be drawn is as the road range increases the hydrogen tank increases which lead to an increase in the total cost and the car mass.

Table 5.7: Simulation results for test run 4

<b>Run Number</b>	<b>Hydrogen Tank Size (g)</b>	<b>Fuel cell Size (kW)</b>	<b>Battery Size (kWh)</b>	<b>Investment Cost (\$/yr.)</b>	<b>Operation Cost (\$/yr.)</b>	<b>Total Cost (\$/yr.)</b>	<b>Car Mass (kg)</b>
6	12000	35	10	2529	404	2933	1642
11	13000	35	10	2555	406	2961	1651
12	12000	30	11	2545	428	2973	1639
10	12000	25	11	2524	450	2974	1628
16	13000	40	10	2576	398	2974	1662
18	12000	35	11	2567	413	2980	1650
8	12000	20	11	2502	486	2988	1617
20	14000	35	10	2581	408	2989	1660
25	14000	50	9	2607	384	2991	1685
21	13000	30	11	2571	430	3001	1648
27	14000	40	10	2602	400	3002	1671
19	13000	25	11	2550	453	3002	1637
30	13000	35	11	2593	416	3009	1659
34	15000	35	10	2607	410	3017	1669
15	13000	20	11	2528	489	3017	1626
38	14000	45	10	2624	394	3018	1682
				:			
				:			
36	12000	5	12	2476	949	3425	1592
22	6000	5	14	2396	1049	3445	1554
44	10000	5	13	2462	1005	3467	1582
45	5000	5	15	2408	1109	3517	1553

#### 4. Test run 5

In this test run the gradeability effect on the UDDS driving cycle will be removed in order to study the effect of 5% slope on the whole (HWFET) Driving Cycle.

Table 5.8: Simulation results for test run 5

Run Number	Hydrogen Tank Size (g)	Fuel cell Size (kW)	Battery Size (kWh)	Investment Cost (\$/yr.)	Operation Cost (\$/yr.)	Total Cost (\$/yr.)	Car Mass (kg)
1	15000	25	8	2487	904	3391	1631
2	15000	25	9	2525	952	3478	1639
5	15000	25	10	2564	1002	3566	1647
9	15000	25	11	2602	1052	3655	1655
14	15000	25	12	2640	1104	3745	1663
19	15000	25	13	2679	1157	3836	1670
28	15000	25	14	2717	1211	3928	1678
12	12000	20	13	2579	1357	3936	1633
16	13000	20	13	2605	1368	3973	1642
17	14000	20	13	2631	1379	4010	1651
34	15000	25	15	2756	1266	4022	1686
21	15000	20	13	2657	1390	4047	1659
18	12000	20	14	2617	1433	4050	1641
22	13000	20	14	2643	1444	4088	1649
25	14000	20	14	2670	1456	4126	1658
29	15000	20	14	2696	1468	4164	1667

As shown from the comparison table if 5 % slope added to the HWFET the fuel cell size becomes larger than the design without gradeability and smaller than the design with gradeability. However, the total cost of (c) is higher than (a) and (b) since the battery and hydrogen tank sizes are bigger than both. While the car mass is larger than (a) and (b) since the hydrogen tank increases to 15 kg.

Table 5.9: Comparison table for the best design

	Hydrogen Tank Size (g)	Fuel cell Size (kW)	Battery Size (kWh)	Investment Cost (\$/yr.)	Operation Cost (\$/yr.)	Total Cost (\$/yr.)	Car Mass (kg)
A	8000	45	9	2429	376	2805	1620
B	5000	10	4	2007	306	2314	1478
C	15000	25	8	2487	904	3391	1631

- a) Base case
- b) Test run 3

c) Test run 5

### 5. Test run 6

This test run is done to verify that there is no difference between the different selection methods of the OO. The best good enough solution are the same. The selection method used in this section is based on plotting the ordered performance curve OPC. After testing the crude model, the performances of the feasible designs are sorted from the lower to the higher cost then plotted with respect to the order. The OPC curve for the same conditions of the base case is shown in Figure 5.6. The obtained OPC is the bell curve. This curve means that many mediocre designs exist. The number of the top- $S$  is 20 designs. This number is calculated from the column of the bell, row of the minimum error and the equation  $Z(k, g) = e^{Z_1} k^{Z_2} g^{Z_3} + Z_4$  of Table 3.1. Table 5.8 proves that the results with different selection methods are the same.

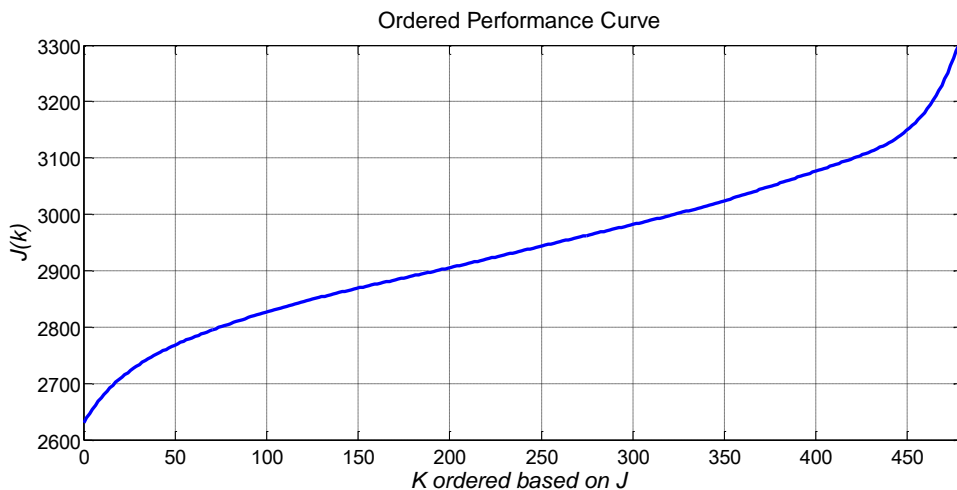


Figure 5.6: Order Performance Curve

## CHAPTER VI

### CONCLUSION

This thesis presents an ordinal optimization approach for finding a good solution to an optimization problem in a large space. The ordinal optimization (OO) in addition to the dynamic program offers an efficient approach to determine the good enough design of the FCHEV power units for the purpose of reducing hydrogen fuel consumption and lowering operation and investment cost. Dynamic programming simulates the operation of the car for a set of specified sizes on the (UDDS) and (HWFET) as mixed driving cycles and provides the total vehicle cost per year. The OO program sets the sizes of the car components to sample the search space using a fast but crude model. Different test runs are done to study the effect of the components' prices and gradeability on the sizes of the fuel cell, battery and hydrogen tank.

Several test runs were carried out based on different variations in the fuel cell cost, the hydrogen cost, the drive cycles gradeability, the car range specification, and the method of selection in the OO approach. In the base case the costs of the fuel cell and the hydrogen were \$45/ kW, \$3/ kg, respectively. The car range was 240 km, and the gradeability was an additional part of a drive cycle added to the UDDS with slope of 5% and top speed of 110 km/h. The selection method was a blind pick. The best feasible design in the base case had hydrogen tank size of 8000 g, a fuel cell capacity of 45 kW, and a battery capacity of 9 kWh. In Test Run 1, the fuel cell cost was set at \$30/ kW and the rest of the parameters were as defined above. The best design in this case had the same unit sizes as the base case. In Test Run 2, the fuel cell and hydrogen costs were set at \$30/kW and \$1.5/kg respectively and the rest of the parameters were as defined in



the base case. The best design obtained had hydrogen tank size of 8000 g, a fuel cell capacity of 30 kW, and a battery capacity of 10 kWh. Test run 1 and 2 had shown that as fuel cell unit cost decreases the investment cost decreases and as the hydrogen cost decreases the operation cost decreases. Test Run 3, the additional gradeability at the beginning of the UDDS was removed and the rest of the parameters were as defined in the base case. The best design had shown a decrease in the unit sizes such as the hydrogen tank size of 5000g, fuel cell capacity of 10 kW, and a battery capacity of 4 kWh. In Test Run 4, the road range was considered 400 km and the rest of the parameters were as defined in the base case. The best feasible design had hydrogen tank size of 12000 g, a fuel cell capacity of 35 kW, and a battery capacity of 10 kWh. In Test Run 5, a gradeability with slope 5% is added for the full and simple HWFET and the rest of the parameters were as defined in the Test Run 3. The best feasible design had hydrogen tank size of 15000 g, a fuel cell capacity of 25 kW, and a battery capacity of 8 kWh. The last test run was done with OO selection method based on the ordered performance curve and the rest of the parameters were as defined in the base case. The obtained results were same as the base case results.

The accurate model can be updated in the future by adding the detailed models of the fuel cell and the battery. In addition to the motor size can be added as fourth variable since as the three sizes – fuel cell, battery and hydrogen tank – change the mass changes too, therefore the motor size will change.

## REFERENCES

- [1] X. Li, J. Li, L. Xu, M. Ouyang, "Power management and economic estimation of fuel cell hybrid vehicle using fuzzy logic", *IEEE*, pp.1749,1754, 7-10 Sept. 2009
- [2] R. Dinnaw, D. Fares, R. Chedid, S. Karaki, R. Jabr, "Optimized Energy Management System for Fuel Cell Hybrid Vehicles", *17th IEEE Mediterranean Electrotechnical Conference* April 2014
- [3] E. Tate and S. Boyd, "Finding Ultimate Limits of Performance for Hybrid Electric Vehicles", SAE technical paper, 2000.
- [4] J. Bernard; S. Delprat; F. Buechi; T.M. Guerra, "Global Optimisation in the power management of a Fuel Cell Hybrid Vehicle (FCHV)," *Vehicle Power and Propulsion Conference, 2006. VPPC '06. IEEE*, pp.1,6, Sept. 2006.
- [5] I.L. Sarioglu; O.P. Klein; H. Schroder; F. Kucukay, "Energy Management for Fuel-Cell Hybrid Vehicles Based on Specific Fuel Consumption Due to Load Shifting," *Intelligent Transportation Systems, IEEE Transactions on*, vol.13, no.4, pp.1772,1781, Dec. 2012
- [6] J. Zhong; M. Xie; F. F. Wu "Ordinal Optimization for Power Systems," *IEEE*, 2006
- [7] R.A. Jabr; B.C. Pal, "Ordinal optimisation approach for locating and sizing of distributed generation" *IET Gener. Transm. Distrib.*, Vol. 3, Iss. 8, pp. 713–723, 2009
- [8] Bernard, J.; Delprat, S.; Buchi, F.N.; Guerra, T.-M., "Fuel-Cell Hybrid Powertrain: Toward Minimization of Hydrogen Consumption," *Vehicular Technology, IEEE Transactions on*, vol.58, no.7, pp.3168,3176, Sept. 2009

- [9] A. Elgowainy, J. Han, L. Poch, M.Wang, A.Vyas, M. Mahalik, and A. Rousseau  
 “Well-to-Wheels Analysis of Energy Use and Greenhouse Gas Emissions of Plug-  
 In Hybrid Electric Vehicles,” *Argonne National Laboratory*, June 2010
- [10] A. Elgowainy, A. Burnham, M.Wang, J. Molburg, and A. Rousseau “Well-to-  
 Wheels Analysis of Energy Use and Greenhouse Gas Emissions of Plug-In Hybrid  
 Electric Vehicles,” *Argonne National Laboratory*, February 2009
- [11] A. Emadi; K. Rajashekara; S.S. Williamson; S.M. Lukic, "Topological overview  
 of hybrid electric and fuel cell vehicular power system architectures and  
 configurations," *Vehicular Technology, IEEE Transactions on* , vol.54, no.3,  
 pp.763,770, May 2005
- [12] A. Elgowainy, M.Wang “Fuel Cycle Comparison of Distributed Power  
 Generation Technologies,” Center of transportation Research, *Argonne National  
 Laboratory*, November 2008
- [13] J. Bauman; M. Kazerani "A Comparative Study of Fuel-Cell–Battery, Fuel-  
 Cell–Ultracapacitor, and Fuel-Cell–Battery–Ultracapacitor Vehicles," *Vehicular  
 Technology, IEEE Transactions on* , vol.57, no.2, pp.760,769, March 2008
- [14] Burke, F. Andrew, "Batteries and Ultracapacitors for Electric, Hybrid, and Fuel  
 Cell Vehicles," *Proceedings of the IEEE* , vol.95, no.4, pp.806,820, April 2007
- [15] V. H. Johnson, “Battery performance models in ADVISOR,” *J. Power Sources*,  
 vol. 110, no. 2, pp. 321–329, Aug. 2002
- [16] HO Y.-C., ZHAO Q.-C., JIAQ.-S., ‘Ordinal Optimization: Soft Optimization for  
 Hard Problems’ (Springer, New York, 2007)

- [17] X. Guan, Y. Ho, and F. Lai ‘An Ordinal Optimization Based Bidding Strategy for Electric Power Suppliers in the Daily Energy Market’ *IEEE TRANSACTIONS ON POWER SYSTEMS*, vol. 16, no. 4, November 2001
- [18] D. Wu; Williamson, S.S. "A novel design and feasibility analysis of a fuel cell plug-in hybrid electric vehicle," *Vehicle Power and Propulsion Conference*, 2008. VPPC '08. IEEE , vol., no., pp.1,5, 3-5 Sept. 2008
- [19] S. Karaki, R. Chedid, R. Jabr, F. Panik ‘Optimal Energy Management of Hybrid Fuel Cell Electric Vehicles’ “not published”
- [20] H. Hongwen, R. Xiong and F. Jinxin “Evaluation of Lithium-Ion Battery Equivalent Circuit Models for State of Charge Estimation by an Experimental Approach,” *Energies Journal* vol. 4, pp. 582-598, 29 March 2011